Effect of Alloying Elements (Mo and Al) on Biomaterials Ti-Ta Shape Memory Alloys

Dr. Sahib M. Al-Saffar
Materials Engineering Department, University of Technology/Baghdad
Dr. Emad S. Al-Hassani
Materials Engineering Department, University of Technology/Baghdad
Fatima J. Al-Hassani
Materials Engineering Department, University of Technology/Baghdad
Email: uot_magaz@yahoo.com

Received on: 10/4/2012 & Accepted on: 5/12/2013

ABSTRACT

Titanium-Tantalum shape memory materials have widespread potential in biomedical applications In this research the alloy of (Ti-Ta) has been prepared by powder metallurgy technique use fixed percentage of Ta (30 at%), then the alloying elements (Mo and Al) has been added in different compositions (1 at%, 2 at% and 3%) to the master alloy (70% Ti -30% Ta) in order to improve corrosion resistance and mechanical properties . examination were done by using XRD, SEM technique, DSC, Vickers hardness, the porosity percentage and corrosion rate in different solutions (artificial saliva, Ringer solution and blood plasma).The XRD and microstructure results show that all samples with and without additives consist of two phases (β-phase) and (α-phase) at room temperature and the addition of Mo and Al in these percentages does not have effect on present phases. he transformation temperature decreases with the increasing in Mo percentage while this temperature increase with the increasing in Al percentage. The addition of Mo and Al leads to lower the hardness except 3% Mo this sample has highest value than the master sample. The porosity percentage decrease gradually with the increasing in the both Mo and Al percentage due to the better inter diffusion caused by these additives. From the corrosion results in 3% Mo the alloys have less corrosion rate than the master or other percentage (1 at% and 2 at %) In all solutions (artificial saliva, simulated body fluid(Ringer solution) and blood plasma) but the Al has a good corrosion rate in (artificial saliva and blood plasma).

Keywords: Ti-Ta Alloy, Shape Memory Alloys, Biomaterial, Corrosion Resistance.

تأثير إضافة العناصر السبائكية على سبيكة ذاكرة الشكل Ti-Ta الطبية الإحيائية

الخلاصة

أن السبائك ذات الذاكرة تعتبر من المواد المهمة التي تستخدم في التطبيقات الطبية كالزراعة الطبية الحيوية وذلك لما تمتاز به من مقاومة تأكل ,المرونة الفائقة إضافة إلى التوافقية العالية داخل الأجسام الحية. ولذلك ظهرت دراسات لتطوير هذا النوع من السبائك (الخالية من النيكل) ذات أساس من التيتانيوم وعناصر سبائكية غير سامة, حيث تعتبر سبيكة التيتانيوم من السبائك الواسعة الاستخدام

https://doi.org/10.30684/etj.32.4A.10
2412-0758/University of Technology-Iraq, Baghdad, Iraq

خاصة في مجال التطبيقات الطبية الحيوية لأنها غير سامة وإنها ذات درجة عالية من التوافقية الحيوية . في هذا البحث تم استبدال عنصر النيكل السام بعنصر التنتالوم وبنسبة ذرية ثابتة (30%) ثم إضافة العناصر السبائكية (الموليبدنيوم والألمنيوم) بنسب ذرية مختلفة (3%,2%,1%) إلى السبيكة الأساس لدراسة تأثير هذه العناصر على السبائك ذات الذاكرة.أظهرت نتائج حيود الأشعة السينية والبنية المجهرية إن كل العينات (مع الإضافات أو بدونها) تتكون من طورين أساسيين هما الفا وبيتا عند درجة حرارة الغرفة وان إضافة عنصري الموليبدنيوم والألمنيوم بتلك النسب الذرية لا يؤثر على الأطوار الظاهرة في السبيكة الأساس. وكذلك أظهرت النتائج حصول انخفاض في درجة حرارة التحول عند زيادة نسبة الموليبدنيوم والألمنيوم حيث إن درجة حرارة بداية التحول للمارتنسايت انخفضت مقارنة بالسبيكة الأساس وهذا يشير الى إن طور بيتا أصبح أكثر استقرارا مقارنة بالطور الفا مع إضافة العناصر المضافة. كما أوضحت النتائج إن إضافة الموليبدنيوم والالمنيوم يؤدي إلى انخفاض الصلادة والمسامية بالمقارنة مع صلادة ومسامية السبيكة الأساس. ومن خلال نتائج التآكل يمكن ملاحظة إن السبيكة التي تحتوي (3%) موليبدنيوم هي اقل معدل تأكل من السبيكة الأساس و باقي السبائك التي تحتوي على عناصر سبائكية. وأخيرا تم استنتاج أن السبائك ذات الذاكرة من نوع التيتانيوم والتنتالوم مع وجود هذه الإضافات (Mo, Al) تكون ملائمة للاستخدام في جسم الإنسان وفي تطبيقات طب الأسنان.

INTRODUCTION

Shape memory alloys (SMA) are materials that have the ability to return to a former shape when subjected to an appropriate thermo mechanical procedure. Pseudoelastic and shape memory effects are some of the behaviors presented by these alloys. The unique properties concerning these alloys have encouraged many investigators to look for applications of SMA in different fields of human knowledge [1]. SMAs are extensively used in biomedical applications. Orthodontic wires, catheters and intravascular stents are particular examples of medical devices that benefit from the shape memory effect in these unique alloys [2]. Ti-Ta binary shape memory alloys have attracted much interest due to the absence of toxic element and the low Young_s modulus [3]. As well as potential good shape memory alloy properties [4]. The Nb, Ta, Zr, and Sn have been considered excellent b-stabilizing alloying elements for titanium alloys [5]. Which are also biocompatible? Therefore, b-type titanium alloys, such as Ti-35.5Nb-5Ta-7Zr, Ti-29Nb-13Ta-4.6Zr, and Ti-24Nb-4Zr-7.9Sn have been developed as biomedical shape memory and superelastic alloys. Corrosion resistance of Ti-Ta alloys is superior to that of pure Ti, which increases with increase in Ta content [6].

The aim of the present study is to prepare set of Ti-Ta shape memory alloys samples using powder metallurgy technique and study the effect of alloying elements additions such as (Mo &Al) on the hardness, porosity percentage, transformation temperature, and corrosion rate in different solutions artificial such as; saliva, simulated body fluid(i.e. Ringer's solution) and blood plasma.

EXPERIMENTAL WORK

The experimental work includes two main steps:

1. The first step is the preparation of the master sample (Ti-Ta) and the samples with alloying elements (Mo, and Al), as showed in Table (1) by using powder metallurgy technique. The sample preparation includes:
   a- Preparation and mixing of powders.
   b- Compacting of powders.
   c- Make the sintering process at 1000 °C for 9 hours under controlled atmosphere (Argon gas).

2- The second step is the characterization of samples .including the following:-

a- X-ray diffraction (XRD).
b- Differential scanning calorimeter (DSC).
c- Microstructure test (Scanning electron microscope (SEM), optical microscope test).
d- Vickers micro hardness.
e- Porosity measurement.
f- Corrosion rate tests.

Table (1) Alloying element in different percentages to the master samples

Alloying Element	Particle size µm	purity	Percentage at %	Result Alloy at%
Mo	16	99.5	1% 2% 3%	69Ti-30Ta-1Mo 68Ti-30Ta-2Mo 67Ti-30Ta-3Mo
Al	80	99.99	1% 2% 3%	69Ti-30Ta-1Al 68Ti-30Ta-2Al 67Ti-30Ta-3Al

The compaction of the powder of each samples done by using the Punch and die (made from D2 tool steel) with die diameter of 15 mm. and by using the hydraulic press machine type (RAJCO) the powders was pressed under pressure of 850 MPa for 10 min and thus we obtained samples with diameter of 15mm and 4mm in height.

Sintering process was carried out at temperature 1000 °C for 9 hours under controlled atmosphere (argon gas) to impede the samples oxidation. This process was done in two stages in the sintering process due to the inability to make this process in one stage for 9hours so we separated this process for two stages. After sintering process we obtained the Ti-Ta alloys with and without different alloying element.

In order to find out the composition and the phase identification of each sample the XRD test was done by using Shimadzu x-ray diffractometer (XRD - 6000/7000).

DSC is the most widely used technique to determine the transformation temperatures and to get the energy of transformations of shape memory alloys. This test was done by using PL-DSC type. This test conducted by taking (5-10) mg of each sample and testing at scan rate of 15 °C/min. The cooling agent used in the DSC (in order to cool up to -50°C) was liquid nitrogen while maximum temperature was 200°C.

A scanning electron microscope (SEM) is a type of electron microscope that images a sample by scanning it with a high-energy beam of electrons in a raster scan pattern. The electrons interact with the atoms that make up the sample producing signals that contain information about the sample's surface topography, composition, and other properties such as electrical conductivity. The device type is CAM SCAN MV2300. The magnification applied to samples was (50X and 5000X).

The microstructure was studied by optical microscope in order to show the grains and the phases existing, after the samples were ground, polished, and etched in a solution of (8 ml HF, 10 ml $HNO_3$and 82 H_2O); the microscope is type (BEL PHOTONICS).The magnification applied was (200X, 400X, 600X and 800X).

The hardness of these alloys was taken by using Vickers micro hardness tester type (TP µP-A, HV- 1000) where the average of 5 readings was taken. All hardness values were taken at a load of 1Kg.

Due to the use of powder metallurgy method to produce samples, this test is necessary to see the effect of this method on the porosity of samples and the effect of porosity on shape memory property. The porosity percentage was also measured by using Archimedes method. The porosity is measured according to this Formula:

$$\text{Porosity\%} = [(Ws - Wd)\backslash (Ws - Wn)] * 100 \quad \ldots (1)$$

where:

Wd= weight of dry sample (gm).
Ws= weight of saturated samples (gm).
Wn= weight of immersed sample (gm).

Because of the importance of the Ti-base shape memory alloys and their use in important regions within the human body we had make the corrosion test is made on the research samples in order to find out the corrosion behavior of these samples and to determine the period of validity in human body . The device type is X MTD-2MA. In this test we use three different body solutions; artificial saliva, Ringer's solution and synthetic blood plasma as shown in the Table (2):

Table (2) Chemical composition of different body solutions

Solution type	Chemical composition
Artificial saliva[7]	NaCl (0.4g/L), KCl (o.4g/L), $CaCl_2$ (0.78g/L), NaH_2PO_4. H_2O (0.69g/L), Na_2S. $9H_2O$ (0.005g\L), KSCN (0.3g\L), Urea (1g\L).
Simulated body fluid(Ringer's solution)	Adding Ringer tablet to o.5 liter of distillated water and heating the solution to temperature 120°C for 15 min. and leaving it to cool .then Na_2HCo_3 was added to obtain pH of 7.4.Ringer tablet was obtained from Merck Company Germany.
Synthetic blood plasma [8]	NaCl (6.8g\L), KCl(0.4g\L), $CaCl_2$(o.2) $NaHCO_3$ (2.2g\L), Na_2HPO_4 (1.126g\L), NaH_2PO_4 (0.026g\L), $MgSO_4$ (0.1g\L).

The corrosion test was conducted on the samples at temperature 37°C with 1.76 Cm^2 in area. The test was conducted in these steps:

1. Determination of the OCP (open circuit potential) of each sample in the three different solutions, the open circuit potential measurement was maintained up to5 minute with reading every10 second.
2. Calculation of corrosion rate by using this formula:[9]

$$Rmpy = 0.13 * i_{corr.} * eq_{alloy} / \rho_{alloy.} \quad \ldots (2)$$

Where:

i_{corr}: current density of alloy ($\mu A.cm^{-2}$).
eq: Equivalent weight of alloy (g).
ρ: alloy density ($g.cm^{-3}$).

Results and Discussion

X-Ray Diffraction

An X-ray diffraction test was done on all samples after the sintering process. The phases produced as a result of the sintering process can be seen in figure (1), there are probably no pure metals present which prove that the sintering time and temperature used in this work result in complete sintering reaction. X-ray diffraction showed that all the sample alloys consist mainly of two phases (α + β) biphasic structure; Titanium is an allotropic element; that is, it exists in more than one crystallographic form. At room temperature, titanium has a hexagonal close-packed (hcp) crystal structure, which is referred to as "alpha" phase. This structure transforms to a body-centered cubic (bcc) crystal structure, called "beta" phase, at 883 °C (1621 °F)[10].The martensitic phase (α- phase) orthorhombic structure and the austenitic phase (β- phase) B.c.c. structure. It is noteworthy that the volume fractions of β -phase increases along with the increase in alloy Ta content [10-12].

Transformation Temperature

The DSC measurements have been employed, at constant rate of 10 °C/min of heating and cooling cycle for all samples. The measurements are carried out in the temperature range from (-50°C to 200°C). Figure (2) shows the transformation temperature of the master sample, it can see that during the heating cycle has one peak which refers to one phase transformation from 36.0 °C to 44.0°C. While during the cooling cycle of the alloy from austenite to martensite two stage (two peaks) will occur, at temperature (-16.5°C to -16.2 °C and 11.2 °C to 19.9°C). Table (3) and Figures (3-5) show the samples with Mo addition in different percentage of additives. This addition percentage raises the transformation temperature of the alloy during both heating and cooling cycles but this increase in the transformation disappears with increasing the Mo percentage at 3% Mo, the alloy has one phase transformation during the cooling cycle only this is because the Mo is beta stabilized element and this element lowers the beta transition temperature. The beta transition is defined as the lowest equilibrium temperature at which the material is 100% beta. Two groups of elements stabilize the beta crystal structure by lowering the transformation temperature. The beta isomorphous group consists of elements that are miscible in the beta phase, including molybdenum, vanadium, tantalum, and niobium. [10] The other group forms eutectoid systems with titanium, having eutectoid temperatures as much as 333 °C (600 °F) below the transformation temperature of unalloyed titanium.

Table (3) The transformation temperature for samples with additives.

Addition percentage at%	Mo addition				Al addition			
	Heating °c		Cooling °c		Heating °c		Cooling °c	
	As	Af	Ms	Mf	As	Af	Ms	Mf
1 at%	85.5	85.5	17.1 103.1	27.5 109.8	35.9	47.9	-17.3 13.5	-8.8 23.6
2 at%	76.2	76.2	25.9	33.4	43.7	55.2	7.7	18.8
3 at%	---------	-----	8.2	13.6	39.7	49	12.4	21.5

Figures (6, 7, 8) show the sample with Al addition. Compared with the master sample the increase in Al percentage cause increase in the transformation temperature for both heating and cooling cycle, but this alloying element has the opposite effect

compared with Mo because Al is alpha stabilized element. Alloying elements that favor the alpha crystal structure and stabilize it by raising the beta transition temperature include aluminum, gallium, germanium, carbon, oxygen, and nitrogen [10].

Scanning Electron Microscopy

Figures (9 to 22) show the microstructure results (SEM, and optical microstructure) of all samples (master sample and samples with additives).The SEM and optical microscope micrographs is observed after the samples were ground by SiC emery paper with different grits starting from 600,800,1000 grit to get flat and scratch free surface. Finally, these samples were polished with smooth cloth. The etching solution of SEM and optical microscope test was listed in Table (4).

Table (4) Etching solution of SEM and optical microscope test.

Type of test	Solution composition
Scanning electron microscope test	Hydrofluoric acid (HF) 10 ml Nitric acid(HNO_3) 20 ml H_2O 150ml
Optical microscope test	Hydrofluoric acid (HF) 8 ml Nitric acid(HNO_3) 20 ml H_2O 82 ml

The microstructure reveals that all the sample alloys has consist mainly of two phases ($\alpha + \beta$) structure at room temperature as shown in Figures (9 to 22), compared with the master sample, the addition of Mo element lead to increasing the dark reign (β- phase) due to the effect of Mo as the Beta stabilizer elements. This fact is similar to in alpha-beta and beta alloys, some equilibrium beta is present at room temperature. A non-equilibrium, or metastable, beta phase can be produced in alpha-beta alloys that contain enough beta-stabilizing elements to retain the beta phase at room temperature on rapid cooling from high in the $\alpha + \beta$ phase field. One hundred percent beta can be retained by air cooling beta alloys. The decomposition of this retained beta (or martensite) is the basis for heat treating titanium alloys to higher strengths. [10].where by the addition of Al element lead to increasing in the light region due to the effect of Al as α stabilizer element.

Vickers Micro hardness

The measurement of hardness has been done by taking the average of five readings. The results obtained are represented graphically in figure (23). Measurement hardness value of master sample is higher than that of samples with additives except sample with 3% Mo addition. This drop in hardness may be attributed to some phases and pores localized on the surface and can be attributed to the fact that the sample has more porosity than master sample. We can also see that the measurement hardness increases by increasing Mo and Al additives which could be attributed to the melting of Al additives during sintering process which leads to close some pores.

Porosity

The porosity percentage of samples was done by using Archimedes method. The obtained results are represented graphically in figures (24). the porosity percentage decreases with increasing the percentages of Mo and Al additives (1, 2and 3 at%)

respectively which could be attributed to the better interdiffusion caused by the addition. it is also obvious that the porosity percent of the samples when compacted at 850 MPa which is in good agreement with the expectation; since the compacting pressure leads to good adhesion and interdiffusion between the particles is better which results in more elimination of pores.

Corrosion Test Results

The corrosion test was done by using the potentiodynamics polarization test in three different solutions (artificial saliva, simulated body fluid (Ringer's solution), and blood plasma) on the master sample and the samples with Mo, Al additions at temperature 37ºC. The results show that the Ti-30% Ta alloy have good corrosion rate due to the formation of two stable oxide layers (TiO_2 and Ta_2O_5).

This is agreeing with the fact of the corrosion resistance of a pure metal or an alloy strongly depends on the environment where it is exposed, the chemical composition, temperature, velocity and so forth. The excellent corrosion resistance of pure Ti and its alloys results from the formation of very stable, continuous, highly adherent, self- rehealed and protective oxide films (mainly TiO_2) on metal surfaces within milliseconds in a wide range of corrosive media with all pH ranges, and the outstanding corrosion capacity of Ta and its alloys are by contrast because of the formation of the protective oxide films (mainly pentoxideTa_2O_5) [13-15]. Thus, thoseTiO_2 andTa_2O_5 oxide films can definitely result in the expected superior corrosion resistance of Ti–Ta alloys. The data listed in Table (5, 6,and 7) show The E_{corr} which is an indicator of the stability of surface Conditions. Thus, less variability in E_{corr} values from different samples is indicative of more consistent surface processing. The I_{corr} and calculated CR are relative measures of corrosion and illustrate how much of a material will be lost during the corrosion process. Hence, the higher I_{corr} and calculated CR, cause more material lost. Figure (25) show the corrosion behavior and the corrosion rate of all samples in artificial saliva this figure show that the corrosion rate of samples decrease with increasing (Mo, Al) addition ,this refer that the release of metallic ions was inhabit by these additions so the oxides layer became more stable with the increasing in alloying addition, These results show the possibility of using Ti-Ta alloys in the dentistry. Figure (26) show the corrosion behavior and the corrosion rate of all samples in simulated body fluid (Ringer's solution), this Figure show that the corrosion rate of samples with Mo addition decrease with the increasing of Mo percent due to the stability of oxides is modified by increasing in Mo addition ,but the corrosion rate of samples decreases with the increasing in Al in all percentage(1%,2%,3%),this refer to that the composition of the surface oxide film changes according to reactions between the surfaces of metallic materials and living tissues. Even low concentration of dissolved oxygen, inorganic ions, proteins, and cells may accelerate the metal ion release. Figure (27) show the corrosion behavior and the corrosion rate of all samples in blood plasma, this figure show slightly increasing in corrosion rate of samples with Mo, Al addition (1%,2%)compared with the master sample but this increase was draw back with the increase in Mo, Al (3%) this is refer that the concentration of the blood plasma solution effect on the stability of oxide layer in this percentage which lead to increasing in corrosion rate ,but The regeneration time of the surface. Oxide film after disruption also decides the amount of ions released. So the increasing in the Mo, Al lead to modify the regeneration time and stability of oxide layer.

CONCLUSIONS

From studying the effect of alloying elements (Mo and Al) on the Ti-Ta base shape memory alloys the following conclusion can be drawn:

1- All the samples with and without additives were compacted at 850Mpa. The sintering temperature 1000 °C, is very satisfying because elemental powders are completely transformed in to alloy structure.

2- All the samples with and without additives consist of two main phases (β-phase) and (α-phase),this is obtained from XRD and microstructure observations, and the addition of Al and Mo in 1%, 2% or 3% does not cause adding or removing any new phases.

3- The addition of Mo in 1%, or 2% does not have significant an effect on the transformation temperature but from 3%Mo addition, it begins to have effect on the transformation temperature by decreasing it, also the addition of Al increase the transformation temperature in all percentages.

4- The addition of Mo and Al reduces the hardness of the alloy compared with the master sample.

5- The porosity percentage decreases with increase in Mo and Al percentage.

6- The corrosion rate decreases with increase in Mo percentage in all solutions (artificial saliva, simulated body fluid (Ringer solution) and blood plasma). The addition of Al causes increase in corrosion rate in Ringer solution but this addition reduces the corrosion rate in both artificial saliva and blood plasma.

REFERENCE

[1].Machado L.G. And Savi M.A., "Medical applications of shape memory alloys", Brazilian Journal of Medical and Biological Research, 36:683-691, (2003).

[2].Kauffman, G,Mayo , I. memory metal. Chem matters Oct.1993.

[3]. Tong,Y.X. B. Guo, Y.F. Zheng, C.Y. Chung, and L.W. Ma "Effects of Sn and Zr on the Microstructure and Mechanical Properties of Ti-Ta-BasedShape Memory Alloys", 20:762–766, (2011).

[4].P.J.S. Buenconsejo, H.Y. Kim, H. Hosoda, and S. Miyazaki, "Shape Memory Behavior of Ti-Ta and its Potential as a High-Temperature Shape Memory Alloy", Acta Mater. 57(4),p 1068–1077,2009.

[5].E. Eisenbarth, D. Velten, M. Muller, R. Thull, and J. Breme, "Biocompatibility of [Beta]-Stabilizing Elements of Titanium Alloys", Biomaterials, 25(26), p 5705-5713, 2004.

[6].S.J. Li, T.C. Cui, Y.L. Hao, and R. Yang, "Fatigue Properties of a Metastable [Beta]-Type Titanium Alloy with Reversible Phase Transformation,"Acta Biomater, 4(2), p 305–317, (2008)

[7].Geis- Gerstofer J and Waber H, "effect of potassium thiocyanate on corrosion behavior on non-precious metal dental alloys", Dtsch Zahnraz H, 40:87-91, 1985.

[8].Sella.C,J.C Martin, Leocoeur.J, Le Chaun A.,Harmand. MF, Naji.A and Davidas.JP, "biocompatibility and corrosion resistance in biological media of hard ceramic coatings sputter deposited on metal implants", materials. Sci. and Eng., vol.139, pp.49-57, 1991.

[9].Zaki Ahmad, "Principles of corrosion engineering and corrosion control", 2006, Ch.1, pp.2.

[10].George F. Vander Voort, "Metallography and Microstructures", ASM Handbook, Volume 9, 2004.

[11]Gordin DM, Delvat E, Chelariu R, Ungureanu G, Besse M and Laille´ D, "Characterization of Ti–Ta alloys synthesized by cold crucible levitation melting", Adv Eng Mater10:714–9, 2008.
[12].Zhou YL, Niinomi M and Akahori T, " Decomposition of martensite α″ during aging treatments and resulting mechanical properties of Ti-Ta alloys", Mater Sci Eng A ,384:92–101, 2004.
[13].Stern M., Wissenberg H. and Electrochem J., Soc. 106 ,759, 1959.
[14].Davis J.R., "Corrosion Understanding the Basics", ASM International, Materials Park, 2000.
[15].Shreir L.L., F.R.I. C. and F.I. M., "Corrosion of Metals and Alloys", Corrosion, vol. 1:, George Newnes Ltd, 1963.

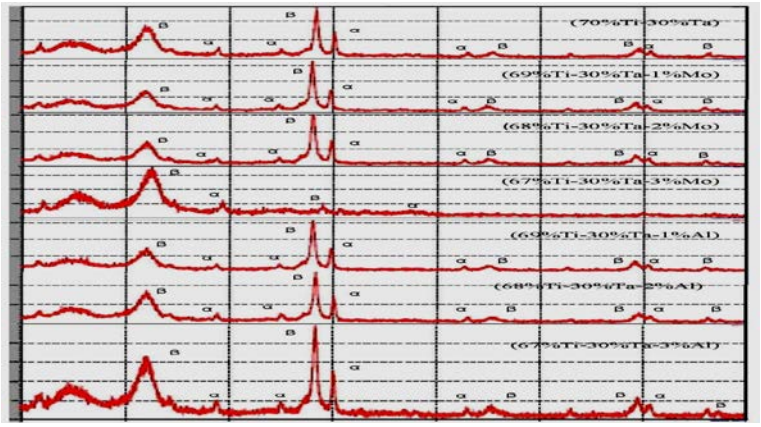

Figure (1) XRD of all samples pressed at 800MPa and sintered at 1000 °C for 9 hrs.

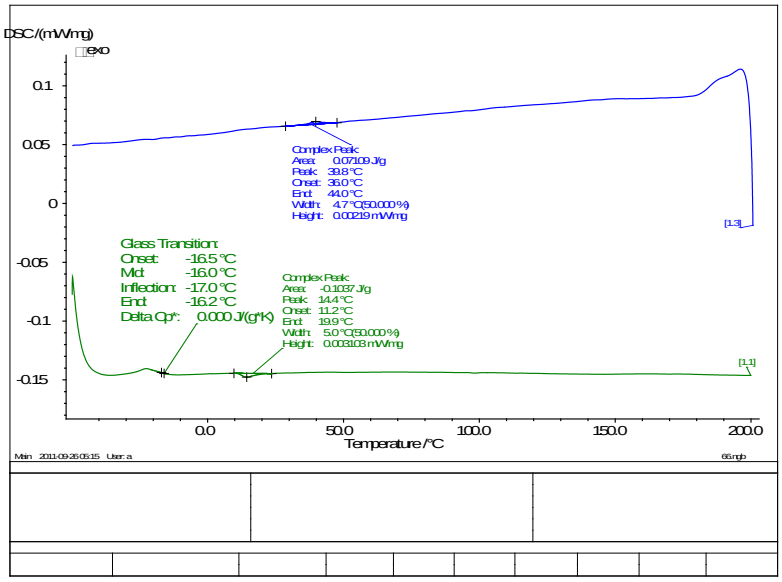

Figure (2) Transformation temperature of master sample (70%Ti-30%Ta).

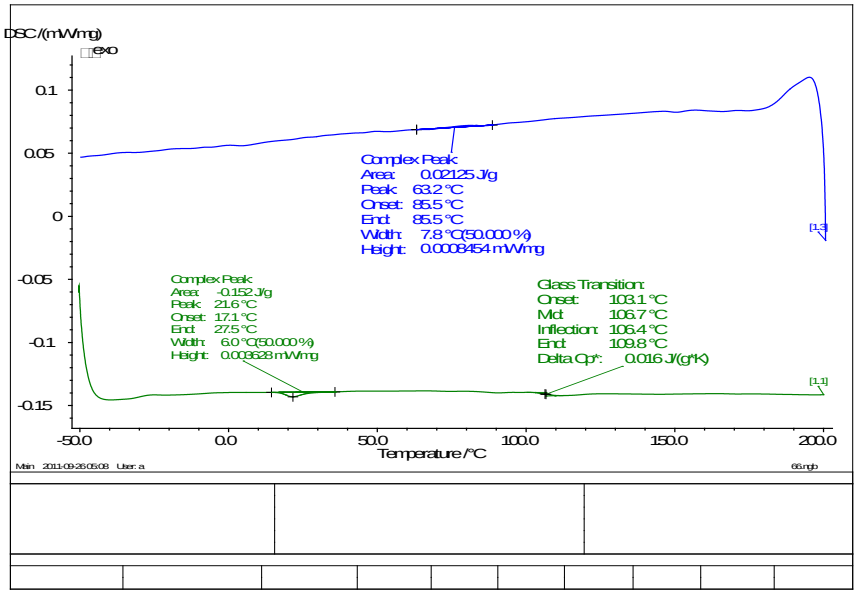

Figure (3) Transformation temperature of (69%Ti-30%Ta-1%Mo).

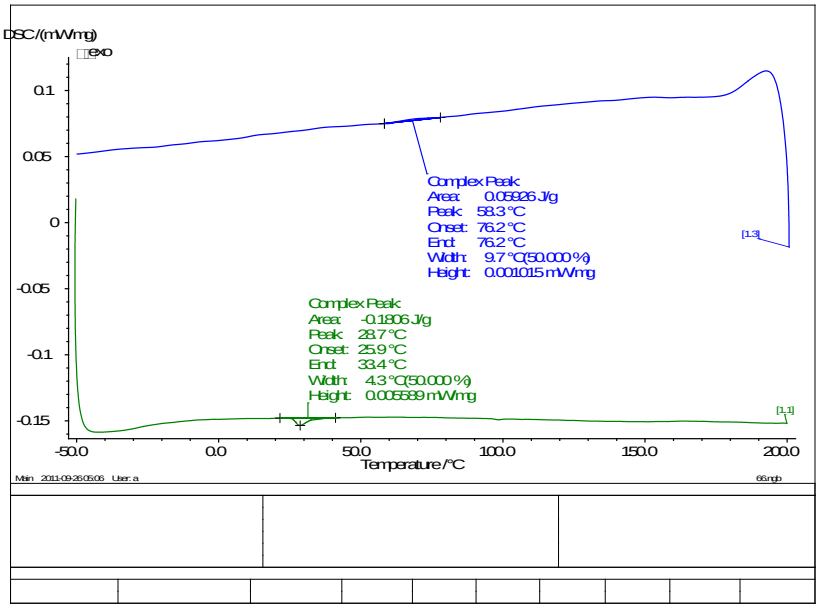

Figure (4) Transformation temperature of (68%Ti-30%Ta-2%Mo).

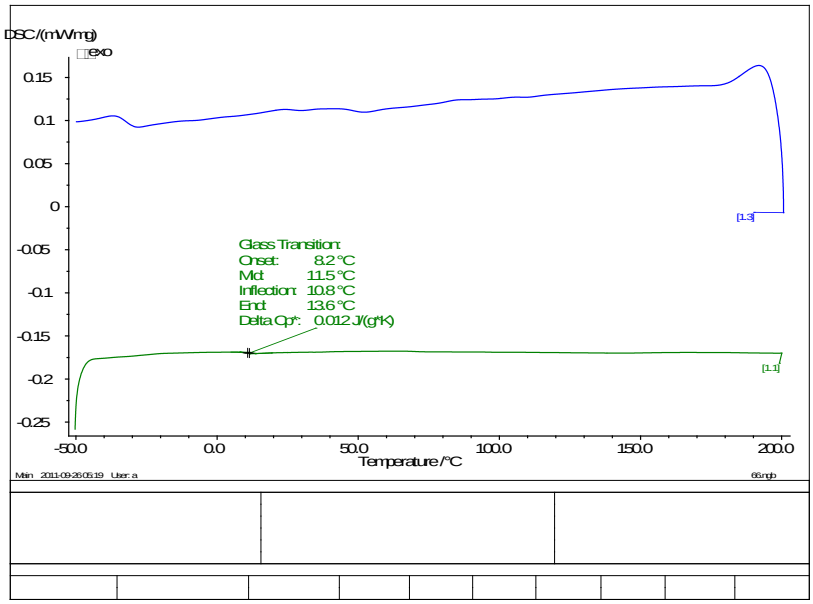

Figure (5) Transformation temperature of (68%Ti-30Ta-3%Mo).

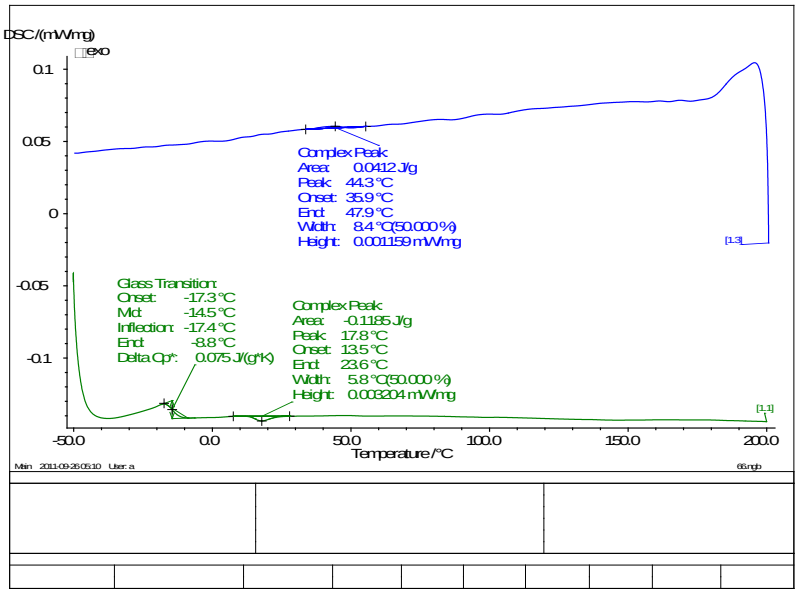

Figure (6) Transformation temperature of (69%Ti-30%Ta-1%Al).

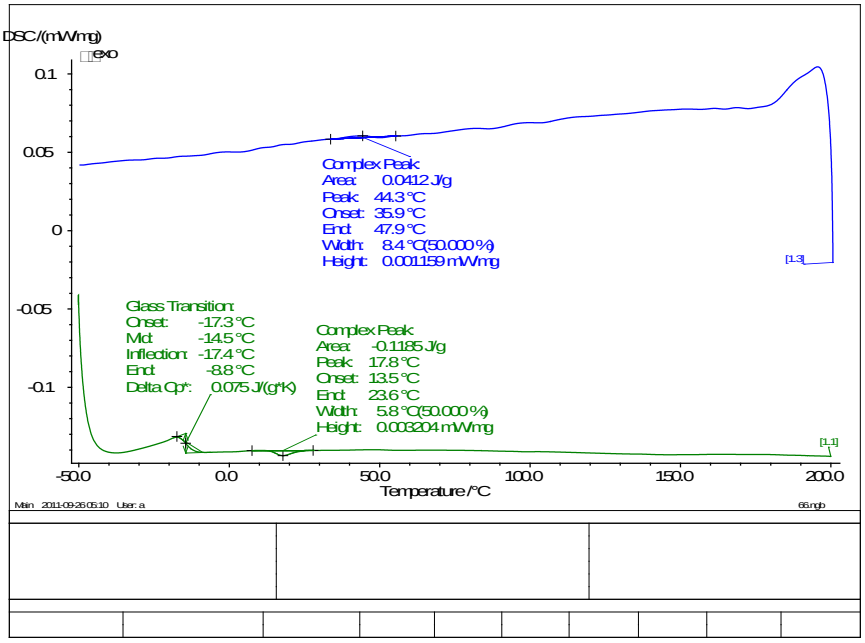

Figure (7) Transformation temperature of (68%Ti-30%Ta-2%Al).

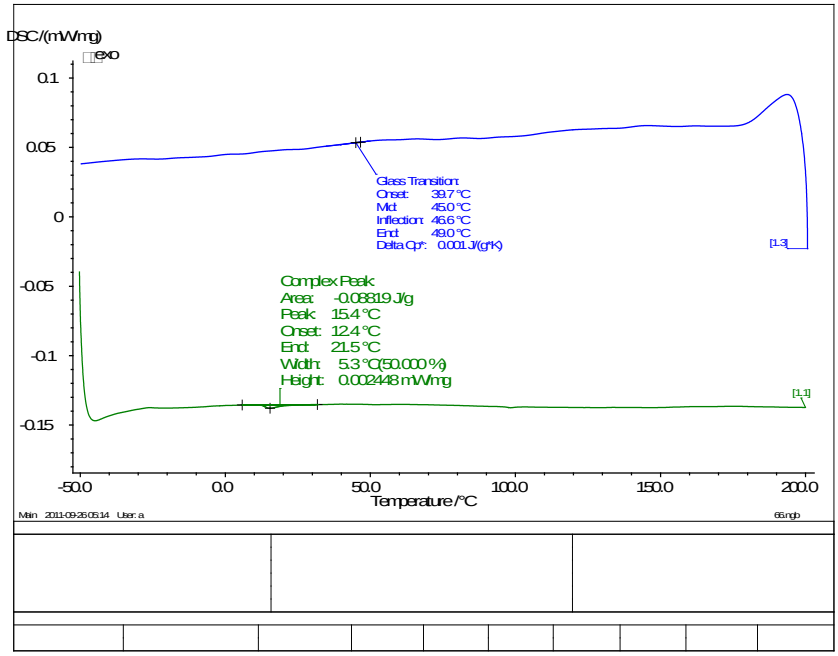

Figure (8) Transformation temperature of (67%Ti-30%Ta-3% Al).

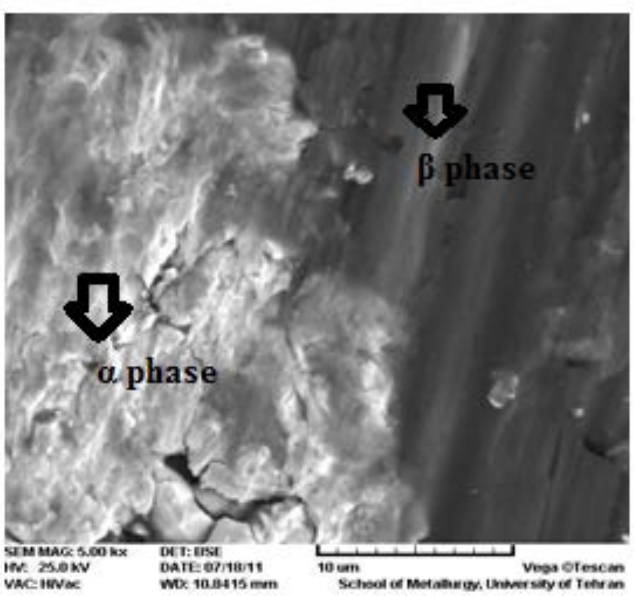

Figure (9) SEM of Master sample (70%Ti-30%Ta).

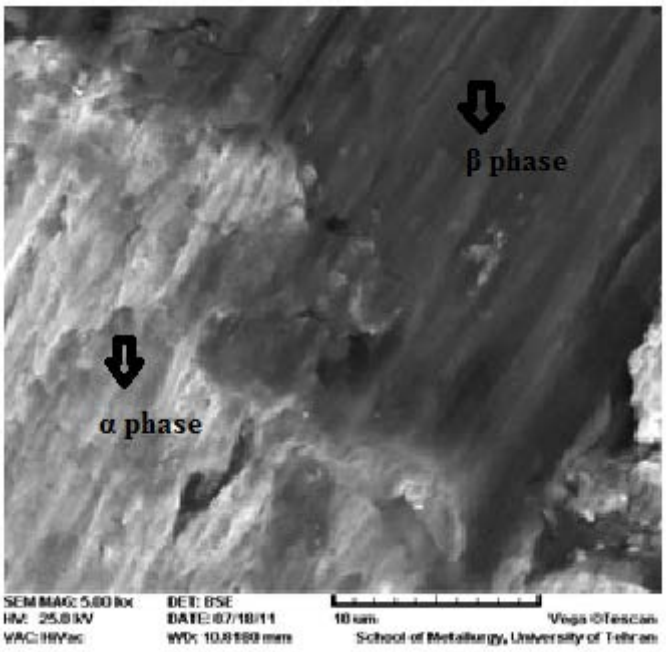

Figure (10) SEM of (69%Ti-30%Ta-1%Mo).

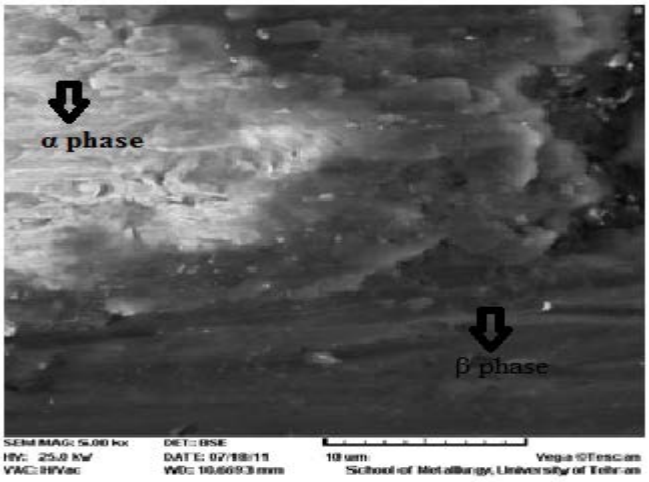

Figure (11) SEM of (68%Ti-30%Ta-2%Mo).

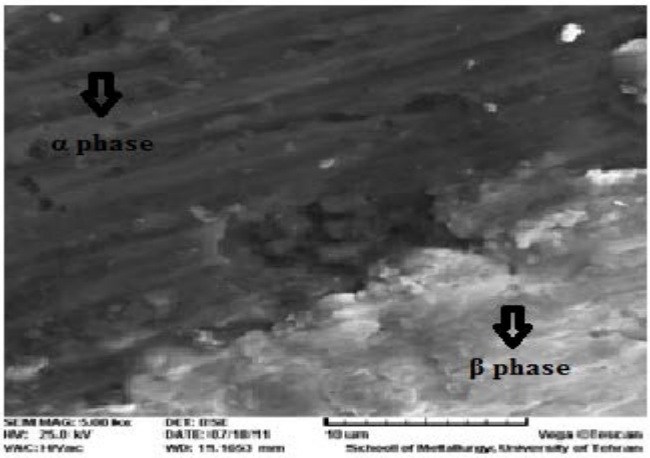

Figure (12) SEM of (67%Ti-30%Ta-3%Mo).

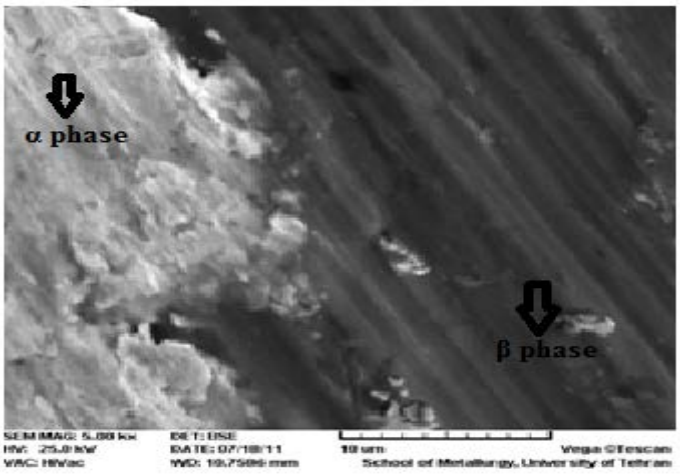

Figure (13) SEM of (69%Ti-30%Ta-1%Al).

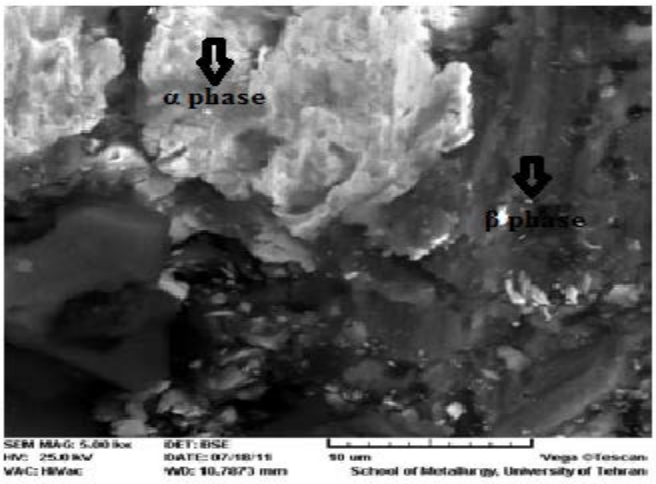

Figure (14) SEM of (68%Ti-30%Ta-2%Al).

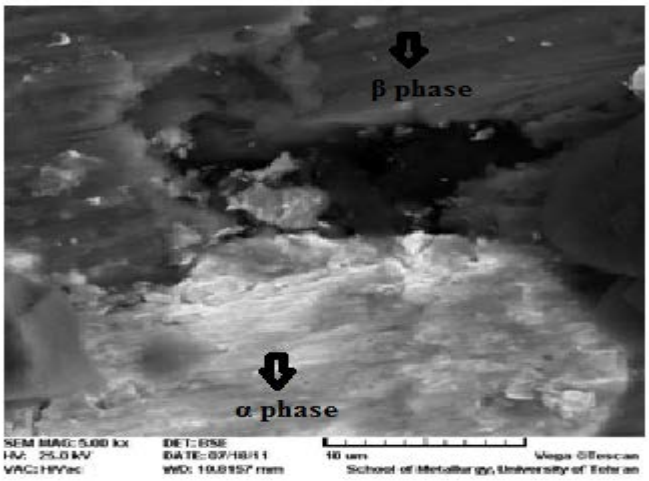

Figure (15) SEM of (67%Ti-30%Ta-3%Al).

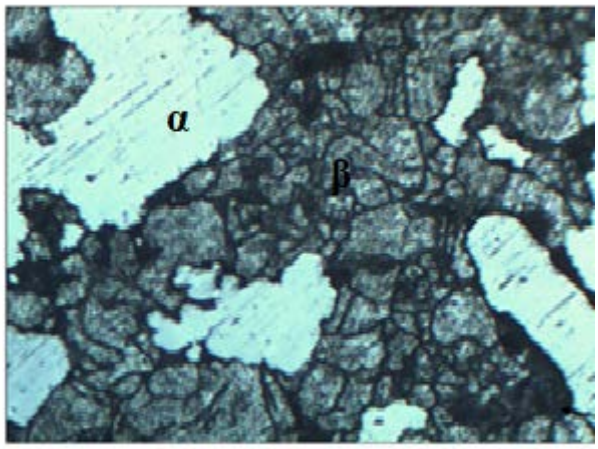

Figure (16) Optical microstructure master sample (70%Ti-30%Ta).

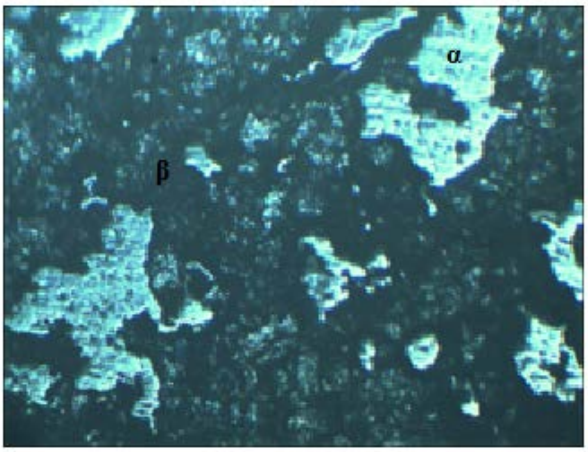

Figure (17) Optical microstructure of sample (69%Ti-30%Ta-1%Mo).

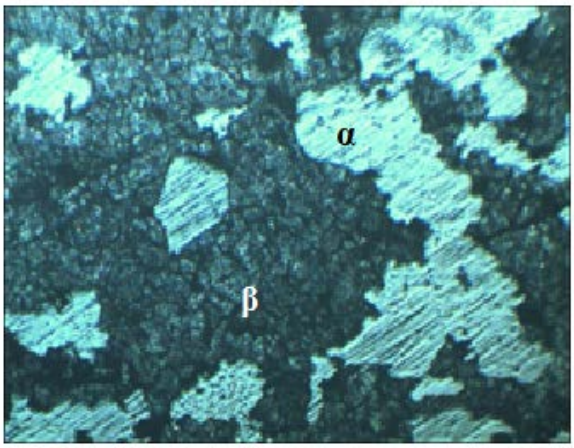

Figure (18) Optical microstructure of sample (68%Ti-30%Ta-2%Mo).

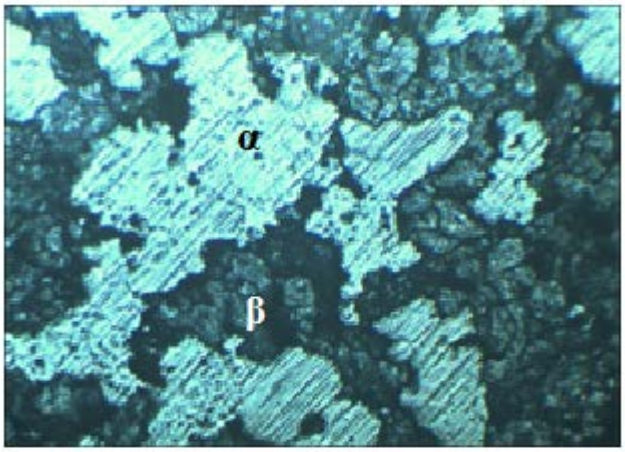

Figure (19) Optical microstructure of sample (67%Ti-30%Ta-3%Mo).

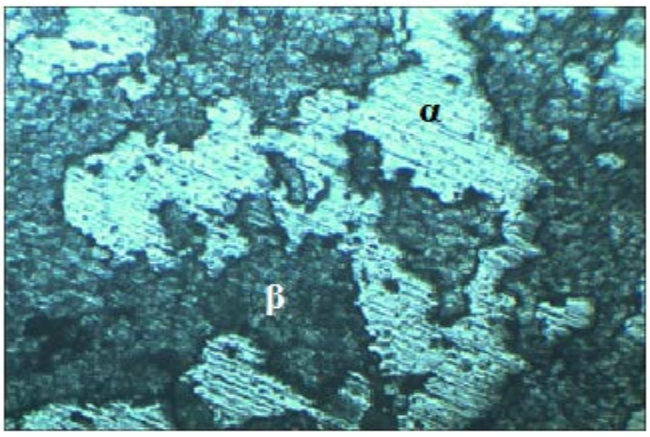

Figure (20) Optical microstructure of sample (69%Ti-30%Ta-1%Al)

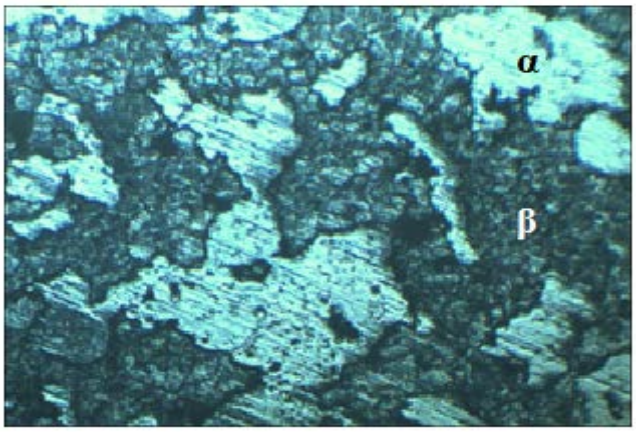

Figure (21) Optical microstructure of sample (68%Ti-30%Ta-2%Al).

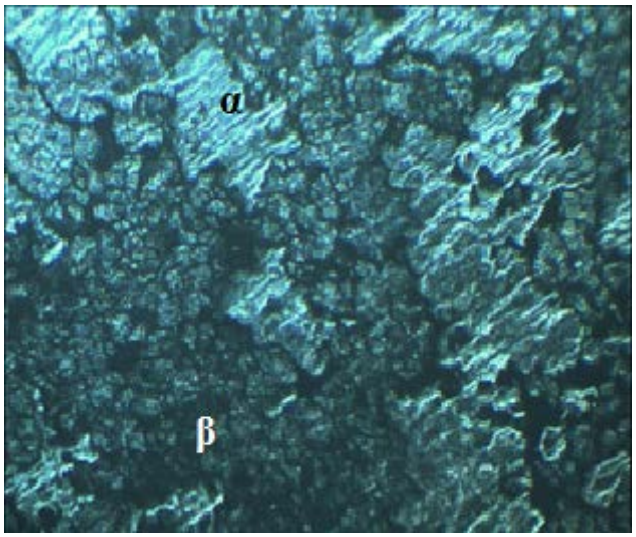

Figure (22) Optical microstructure of sample (67%Ti-30%Ta-3%Al)

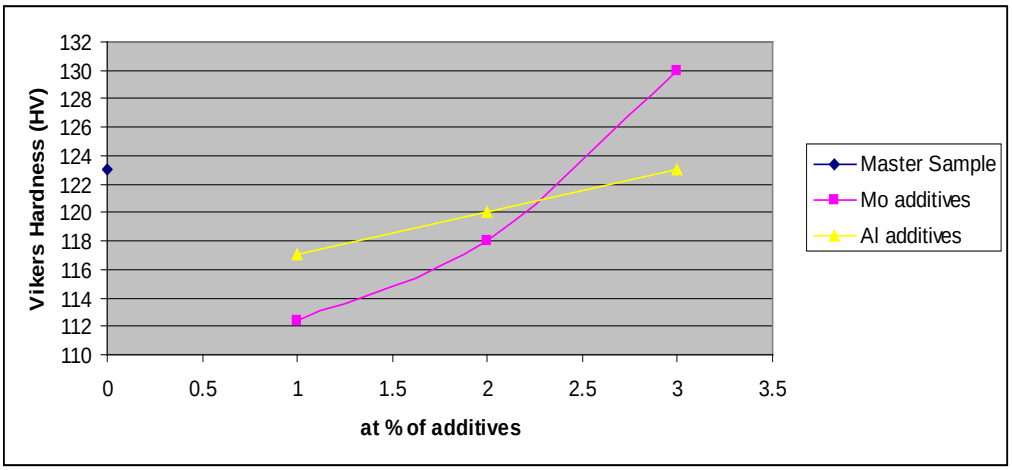

Figure (23) Hardness values for the samples with and without various additives.

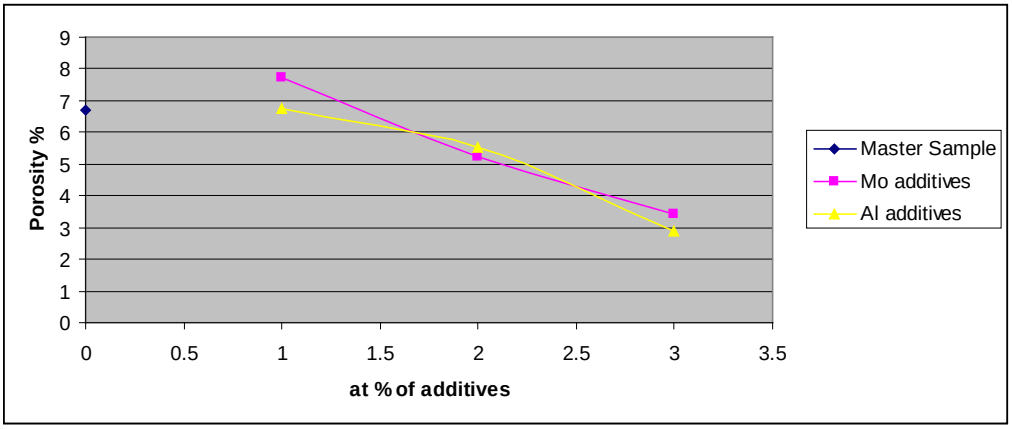

Figure (24) Porosity percentage of the samples with and without various additives.

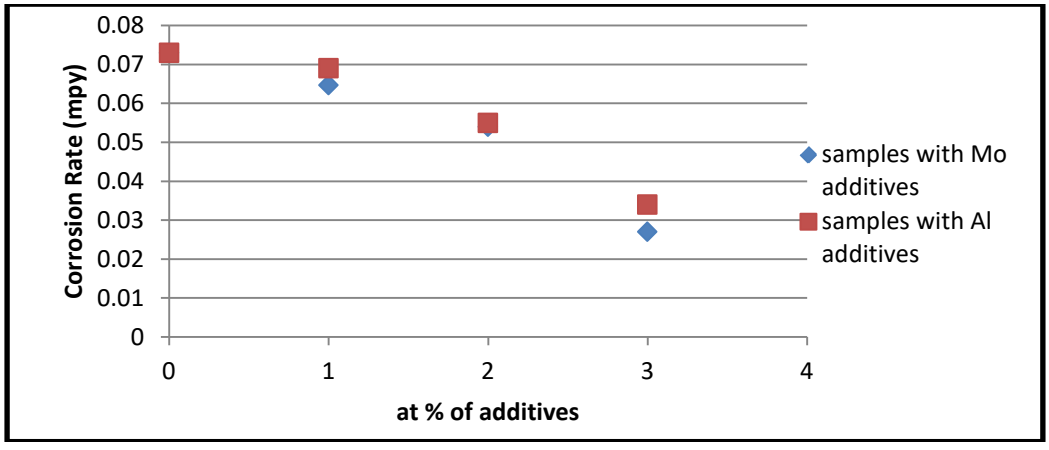

Figure (25) Corrosion rate (mm/yr) of the samples with and without various additives in saliva solution.

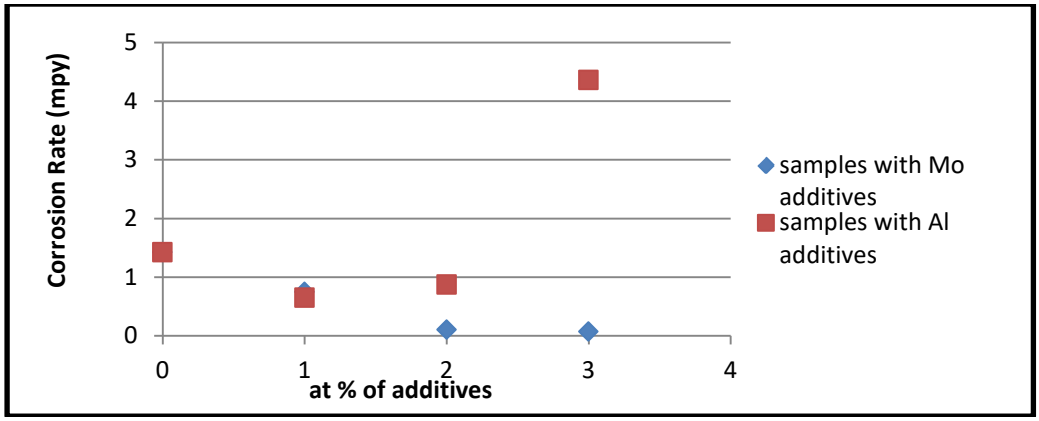

Figure (26) Corrosion rate (mm/yr) of the samples with and without various additives in ringer solution.

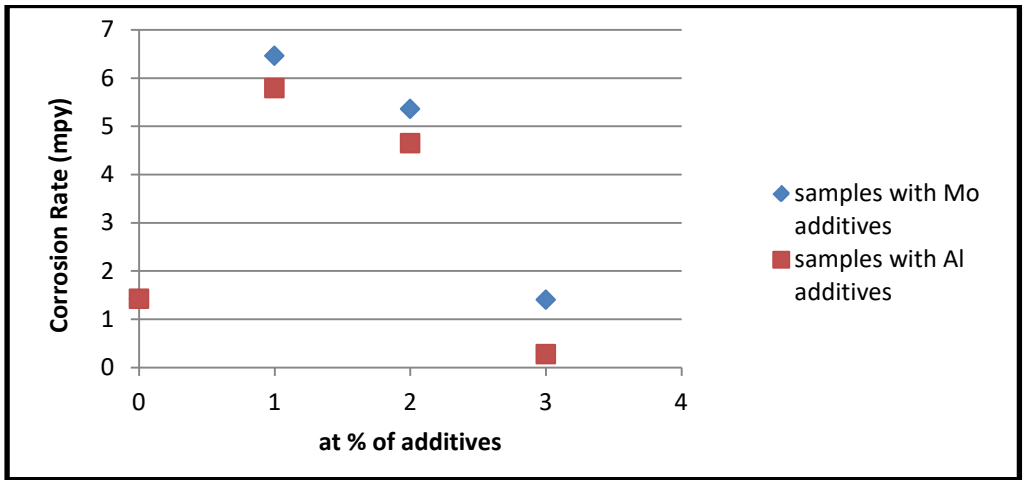

Figure (27) Corrosion rate (mm/yr) of the samples with and without various additives in plasma solution.

Table (5) Corrosion parameters of alloys in artificial saliva.

Alloy composition at%	*-Ocp mV*	*$-E_{corr.}$ mV*	*$i_{corr.}$ $mA.cm^2$*	*$-b_c$ $mv.dec^{-1}$*	*+ ba $mv.dec^{-1}$*	*Corrosion rate mpy ($*10^{-6}$)*
Master(70Ti-30Ta)	312	342.6	0.22	100.4	90.3	0.073
(69Ti-30Ta-1Mo)	111	1.46	15.98	83	115	5.280
(68Ti-30Ta-2Mo)	130	187.5	1.66	65.1	78	0.540
(67Ti-30Ta-3Mo)	147	239	82.16	58	51.3	0.027
(69Ti-30Ta-1Al)	633	600.2	1.79	55.2	56.5	0.373
(68Ti-30Ta-2Al)	618	587.9	1.87	42.9	44.4	0.617
(67Ti-30Ta-3Al)	601	507.6	0.21	19.8	28.9	0.0694

Table (6) Corrosion parameters of alloys in simulated body

fluid (Ringer's solution).

Alloy composition wt%	*-ocp mV*	*$-E_{corr.}$ mV*	*$i_{corr.}$ mA/cm^2*	*$-b_c$ $mv.dec^{-1}$*	*+ ba $mv.dec^{-1}$*	*Corrosion rate mpy ($*10^{-6}$)*
Master(70Ti-30Ta)	144	221.1	4.31	74.7	108.5	1.4240
(69Ti-30Ta-1Mo)	37	98.3	22.94	86.1	111.6	7.4999
(68Ti-30Ta-2Mo)	135	243.0	0.308	58.1	106.0	0.10185
(67Ti-30Ta-3Mo)	188	268.1	0.220	79.6	103.9	0.0729
(69Ti-30Ta-1Al)	88	133.1	1.97	77.9	133.9	0.65098
(68Ti-30Ta-2Al)	94	164.4	2.66	83.1	104.7	0.8789
(67Ti-30Ta-3Al)	690	646.8	13.20	136.3	72.0	4.3619

Table (7) Corrosion parameters of alloys in blood plasma solution.

Alloy composition wt%	*-ocp mV*	*$-E_{corr.}$ mV*	*$i_{corr.}$ mA/cm^2*	*$-b_c$ $mv.dec^{-1}$*	*+ba $mv.dec^{-1}$*	*Corrosion rate mpy ($*10^{-6}$)*
Master(70Ti-30Ta)	437	440.1	4.31	110.4	103.0	1.424
(69Ti-30Ta-1Mo)	127	195.9	19.56	88.2	119.0	6.463
(68Ti-30Ta-2Mo)	86	164.6	60.93	73.7	93.7	20.134
(67Ti-30Ta-3Mo)	635	647.4	4.29	74.3	136.0	1.405
(69Ti-30Ta-1Al)	331	323.2	17.53	121.2	193.5	5.792
(68Ti-30Ta-2Al)	410	441.0	14.07	109.1	169.9	4.649
(67Ti-30Ta-3Al)	679	623.3	0.825	38.7	48.9	0.2727